



OPEN ACCESS

Identification of a protein expression signature distinguishing early from organising diffuse alveolar damage in COVID-19 patients

Helen Ashwin,¹ Luke Milross,² Julie Wilson,³ Joaquim Majo,⁴ Jimmy Tsz Hang Lee,⁵ Grant Calder,⁶ Bethany Hunter,² Sally James,⁶ Dimitris Lagos,¹ Nathalie Signoret,¹ Andrew Filby,⁷ Omer Ali Bayraktar,⁵ Andrew J Fisher,^{2,8} Paul M Kaye ¹

► Additional supplemental material is published online only. To view, please visit the journal online (<http://dx.doi.org/10.1136/jcp-2023-208771>).

For numbered affiliations see end of article.

Correspondence to

Professor Paul M Kaye, University of York, York, UK; paul.kaye@york.ac.uk and Professor Andrew J Fisher, Newcastle University, Newcastle, UK; a.j.fisher@newcastle.ac.uk

HA, LM and JW contributed equally.

Received 10 January 2023
Accepted 9 February 2023
Published Online First
9 March 2023

ABSTRACT

Diffuse alveolar damage (DAD) is the histological expression of acute respiratory distress syndrome and characterises lung pathology due to infection with SARS-CoV-2, and other respiratory pathogens of clinical significance. DAD reflects a time-dependent immunopathological process, progressing from an early/exudative stage through to an organising/fibrotic stage, yet within an individual these different stages of DAD may coexist. Understanding the progression of DAD is central to the development of new therapeutics to limit progressive lung damage. Here, we applied highly multiplexed spatial protein profiling to autopsy lung tissues derived from 27 patients who died from COVID-19 and identified a protein signature (ARG1, CD127, GZMB, IDO1, Ki67, phospho-PRAS40 (T246) and VISTA) that distinguishes early DAD from late DAD with good predictive accuracy. These proteins warrant further investigation as potential regulators of DAD progression.

transcriptomic analyses including spatial transcriptomics have indicated the heterogeneity in the lung response in COVID-19 patients^{6,7} but have not specifically compared DAD at different stages of progression. Thus, proteins associated with progression from EDAD to ODAD remain unclear, a knowledge gap that represents a roadblock to the identification of new therapeutic agents able to prevent progression to pulmonary fibrosis.

To address this question, we examined lung tissue from a cohort of COVID-19 autopsy cases in the UK. We used digital spatial profiling (DSP) to determine differences in protein expression between regions of interest (ROI) identified histologically as EDAD or ODAD. We focused on protein targets with therapeutic potential demonstrated in other diseases and/or preclinical models to identify potential regulators of DAD progression with potential to be rapidly translated in the clinic through drug repurposing.

INTRODUCTION

The COVID-19 pandemic has claimed over 6.6 million lives and despite vaccines that prevent serious illness and use of dexamethasone in severely ill patients, worldwide deaths continue to accrue.¹ There is, therefore, a continued need to identify new treatment options to minimise disease severity. Previous analyses of autopsy cases have identified diffuse alveolar damage (DAD) as a primary histological feature associated with fatal COVID-19.^{2,3}

Based on the analysis of autopsy cases that have succumbed to infection over different time periods, DAD is often represented as a continuum of immunopathology. Soon after tissue insult, early or exudative DAD (EDAD) is characterised by hyaline membrane, fibrin extravasation into the alveoli, pulmonary oedema and the presence of focal interstitial infiltration. Progression to organising DAD (ODAD) is associated with loose areas of fibrosis and commonly chronic interstitial inflammation, whereas in the final stage, fibrotic DAD, dense collagen and thickening of alveolar walls is observed. To date, however, formal evaluation of protein markers associated with inflammation during progression through these stages of DAD have been limited to low-plex immunohistochemistry studies of specific immune cells⁴ or have focused on the alveolar epithelium.⁵ Broader

MATERIALS AND METHODS

Patient samples

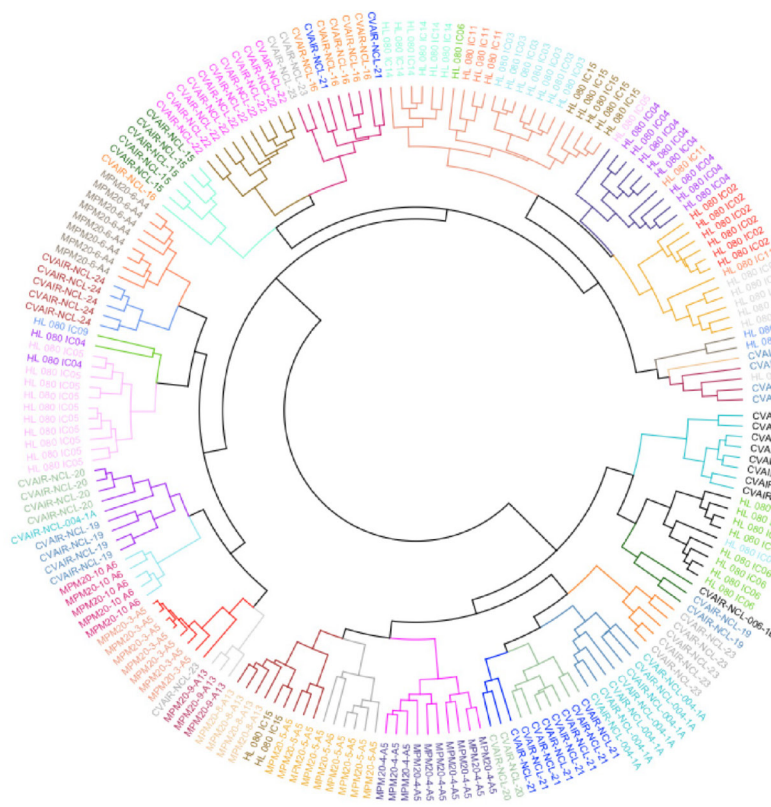
Lung tissue from 27 patients (5 female, 22 male; 7 black/Asian/minority ethnic, 20 caucasian) who had died with SARS-CoV-2 during the first and second wave of the pandemic were selected from a larger cohort assembled by the UK Coronavirus Immunology Consortium (UK-CIC). Prior to death, 7/27 were known to have received steroids, 19/27 antibiotics and 13/27 anticoagulants. None to our knowledge had received treatment with antivirals. Median time from death to post mortem was 3 days (range 1–9 days) (online supplemental table S1). A full description of the UK-CIC cohorts will be provided elsewhere (Milross *et al*, ms in preparation). Patients were selected for the current study based on histological evidence of DAD without concurrent bronchopneumonia or histology attributable to acute cardiac failure. ROIs (approx. 600 µm²) reflecting EDAD, ODAD or a mixed phenotype (MDAD) were identified by a pathologist with cardiothoracic expertise on H&E-stained formalin fixed paraffin embedded (FFPE) sections and used to guide subsequent ROI selection for protein spatial profiling. Patient data relating to pandemic wave, ethnicity, age, sex, illness duration and place of death are provided in online supplemental table S1.



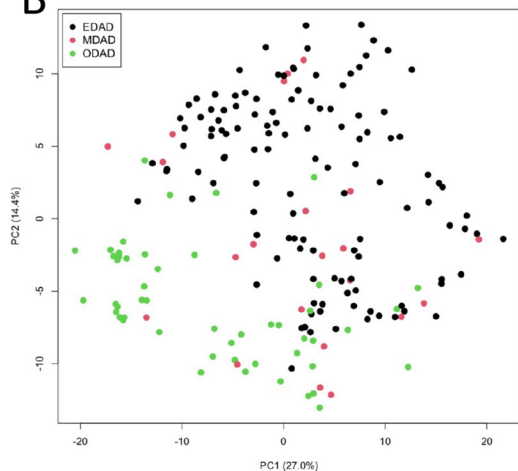
© Author(s) (or their employer(s)) 2023. Re-use permitted under CC BY. Published by BMJ.

To cite: Ashwin H, Milross L, Wilson J, *et al*. *J Clin Pathol* 2023;**76**:561–565.

A



B



C

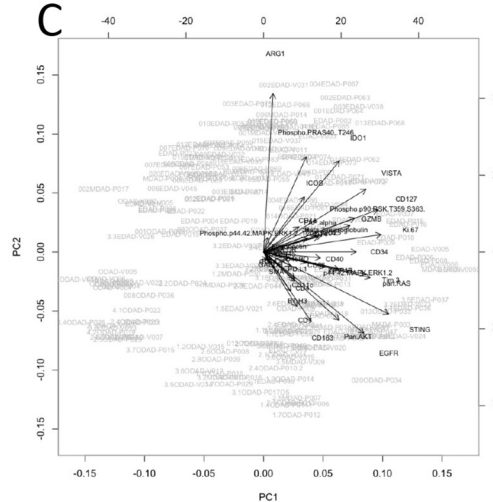


Figure 1 Analysis of protein DSP data. (A) Circular dendrogram from hierarchical clustering of protein DSP ROIs (with patient identifiers colour-coded and clusters coloured separately; see online supplemental table S1). (B, C) Principal component analysis (PCA) scores plot for the first two principal components coloured by EDAD, MDAD and ODAD (B) and with loadings shown as vectors (C). DSP, digital spatial profiling; EDAD, exudative DAD; MDAD, mixed DAD; ODAD, organising DAD; ROI, regions of interest.

Nanostring GeoMx protein spatial profiling

The 4 µm thick FFPE lung sections were used for protein spatial profiling using the Nanostring GeoMx platform. Slides were stained with CD3 and CD68 as morphological markers and with a panel of 68 oligo-nucleotide conjugated antibodies comprising the Immune Cell Profiling Core (24 Abs), IO Drug Target Panel (10 Abs), Immune Activation Status Panel (8 Abs), Immune cell Typing Panel (7 Abs), PI3K/AKT Signalling Panel (9 Abs) and the MAPK Signalling Panel (10 Abs). Regions conforming the histological description of EDAD and ODAD were identified in each patient's lung tissue. ROI capture was performed using a

GeoMx Spatial profiler instrument (Nanostring, Seattle, Washington, USA).

Digital count data were normalised to positive ERCC controls and to housekeeping controls (GAPDH and Histone H3). Housekeeping targets were selected based on high correlation with isotype controls. ROIs with abnormal levels of hybridisation, HK expression or low isotype control background were removed from the analysis. Proteins were thresholded from analysis if signals were below the geometric mean of the isotype controls in >90 of ROIs. Data for the 40 proteins passing QC and thresholding (online supplemental table S1) were exported

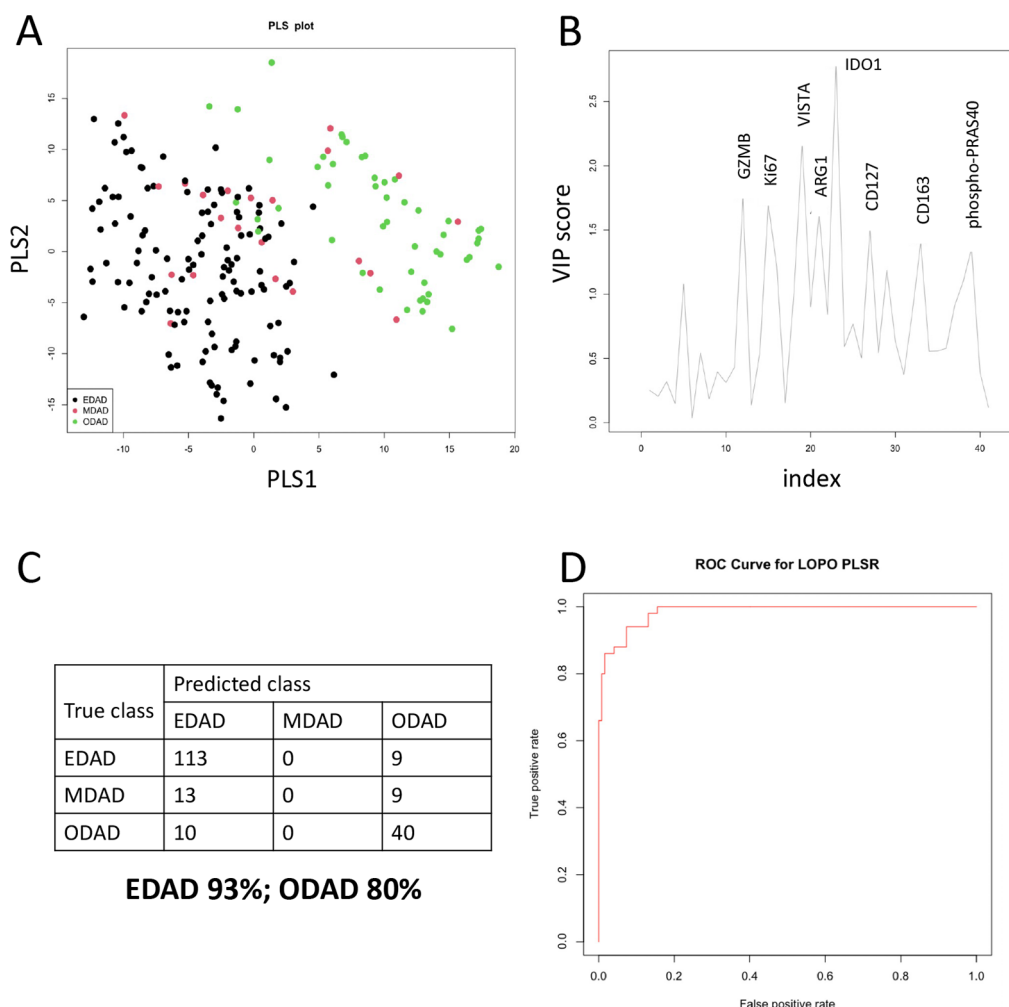


Figure 2 Discrimination of DAD classes based on protein signature. (A, B) Partial least squares analysis of EDAD, MDAD and ODAD samples shown as PLS plot (A) and by variable importance in projection (VIP) score (B). (C) Confusion matrix for results of PLS-LDA leave one patient out prediction using eight variables with VIP scores >1.3 (GZMB, Ki67, VISTA, ARG1, IDO1, CD127, CD163, Phospho.PRAS40). (D) Receiver operating characteristic (ROC) curve generated for EDAD versus ODAD ROIs. DAD, diffuse alveolar damage; EDAD, exudative DAD; LDA, linear discriminate analysis; MDAD, mixed DAD; ODAD, organising DAD; PLS, partial least square; ROI, regions of interest.

for further analysis in R (see Statistical Analysis) and analysed using linear mixed modelling using GeoMx software (V2.0) with patient ID and cohort selected as random variables. Data were analysed using GeoMx software to generate significance scores with false discovery rate (FDR) correction (5%) based on Benjamini, Krieger and Yekutieli two stage setup method and Log2 fold change cut-off of 0.589 (1.5-fold change) between pathology classes. Volcano plots were generated in GraphPad Prism (V9.1).

Statistical analysis

Statistical analyses were carried out in R V4.1.1.⁸ The base R function `prcomp` was used for principal components analysis (PCA), while the `pls` package⁹ was used for partial least squares regression (PLS-R). Classification was performed using the `pls` package¹⁰ with leave-one-patient-out (LOPO) cross-validation to avoid overfitting in this supervised approach. Here, all ROIs for each patient in turn were left out and the remaining data used to build the model which was then used to predict the class of the left-out ROIs. Results are shown for the ROIs that were not used in model training. In order to show the predictive accuracy as the discriminatory threshold was varied, a

receiver operating characteristic (ROC) was generated using the R package `ROCR`.¹¹

RESULTS

We examined 194 ROIs (7 ± 2 ROIs per patient; 122 EDAD, 50 ODAD, 22 MDAD; online supplemental figure S1) for the expression of 40 proteins using GeoMx DSP. As anticipated, we generally observed clustering of ROIs by patient, reflecting repeat sampling (figure 1A and online supplemental table S1). PCA showed separation of each form of DAD with 41.4% of variance accounted for by PC1 and PC2 (figure 1B,C). We next applied PLS-R (figure 2A) and identified variables responsible for group separation using variable importance in projection (VIP) scores. Proteins with VIP scores >1.3 (ARG1, CD127, CD163, GZMB, IDO1, Ki67, phospho-PRAS40 (T246) and VISTA; figure 2B) largely mirrored what was observed with PCA (figure 1C). These eight variables were used to classify ROIs in PLS linear discriminate analysis with LOPO cross-validation to prevent overfitting. This achieved a predictive accuracy of 93% and 80% for EDAD and ODAD, respectively (figure 2C). MDAD ROIs were consistently misclassified, likely a reflection of heterogeneity and the transitional nature of the pathology within this group. Finally,

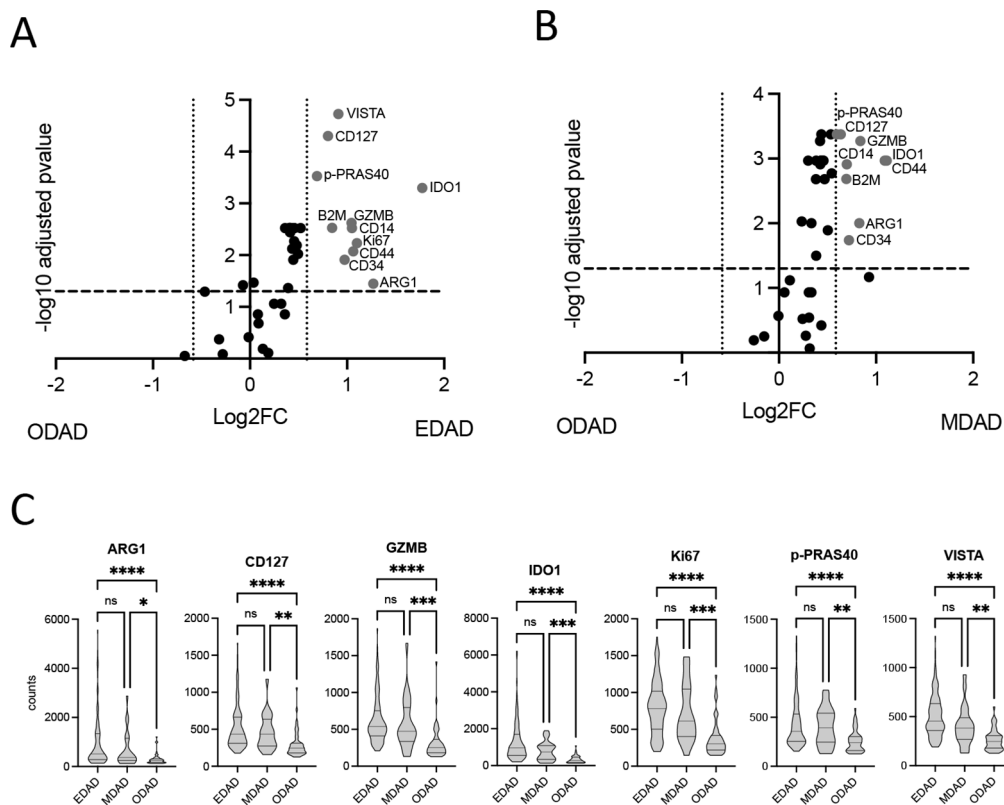


Figure 3 Differential target expression between EDAD and ODAD using linear mixed modelling. (A, B) Differentially expressed (FDR 5%; FC=1.5) protein targets between EDAD and ODAD (A) and MDAD and ODAD (B). Data derives from a linear mixed modelling with patient repeat measures and cohort as a random effect. (C) Individual ROI counts for EDAD, MDAD and ODAD ROIs for identified target proteins. *p<0.05, **p<0.01, ***p<0.001, ****p<0.0001 between indicated groups. ns, non-significant; EDAD, exudative DAD; MDAD, mixed DAD; ODAD, organising DAD; ROIs, regions of interest. FDR, false discovery rate.

we generated an ROC curve for EDAD and ODAD samples using LOPO cross-validation in PLS-R, showing the predictive accuracy as the discriminatory threshold is varied (figure 2D).

We independently analysed these data using linear mixed modelling to account for potentially confounding factors (including repeat measures and cohort effects) and identified eleven targets (ARG1, B2M, CD14, CD34, CD44, CD127, GZMB, IDO1, Ki67, phospho-PRAS40 (T246) and VISTA) distinguishing EDAD and ODAD (>1.5 fold change cut-off, FDR=5%; figure 3A,C). MDAD was similarly distinguished from ODAD (figure 3B,C), but no proteins were significantly different between EDAD and MDAD.

Collectively, our data suggest a core protein signature comprising ARG1, CD127, GZMB, IDO1, Ki67, phospho-PRAS40 (T246) and VISTA distinguishes EDAD from ODAD ROIs in this patient group. Nevertheless, our data also suggest further patient heterogeneity within EDAD ROIs. This was most marked for ARG1, which was absent from all EDAD ROIs in 8/20 patients. Although sample size precluded a formal analysis, this appeared unrelated to sex, place of death, duration of disease, cohort or prior treatment (online supplemental table S1).

DISCUSSION

Using DSP to interrogate well-annotated lung tissue, we identified a core protein signature discriminating early from late phases of DAD. Not surprisingly given the targeted nature of our panel, the proteins we identified have well-known functions in inflammation and immunity, but they have not previously been

evaluated in relation to DAD progression. ARG1 is elevated in the lungs of severe COVID-19 patients, being expressed by CD11b⁺CD66b⁺ granulocytic myeloid-derived suppressor cells.¹² IDO1 has been detected in lung tissue in other autopsy series,^{13 14} and due to its broad expression on endothelial cells, has been implicated in the vasodilation/vasoplegia associated with initial stages of COVID-19 pneumonia.¹⁴ CD127 expression on monocytes has been noted at sites of hyperinflammation,¹⁵ whereas VISTA has been proposed as a therapeutic target to minimise inflammation.¹⁶ A single study found there was a trend for higher GZMB expression to be associated with DAD in patients receiving allogeneic lung transplants.¹⁷

Finally, phosphorylation of PRAS40 at T246 releases mTORC1 to perform its many downstream functions and elevated phospho-PRAS40 (T246) has been used as a biomarker of PI3K/Akt/mTORC1 activation,¹⁸ a pathway implicated in idiopathic pulmonary fibrosis and DAD.¹⁹ While mechanistic studies are required in preclinical models to confirm causality, and possible changes in cellularity need to be considered, the heightened expression in EDAD of proteins associated with mononuclear phagocyte activation suggests that the EDAD-ODAD transition may be associated with dampening of a hyperinflammatory state.

This study has limitations: (1) DSP quantifies protein expression across the entire ROI and cannot distinguish multiple cells with low target expression vs few cells with high target expression; (2) Our patient cohort was too small to perform sub-group analysis based on age, gender, disease duration, place of death or prior treatment; (3) We cannot rule out that patients had other forms of concurrent disease or different forms of DAD in other

areas of lung not sampled here and this may account for some of the inter-patient heterogeneity observed; (4) Further validation is required in an independent patient cohort, preferably incorporating single cell technologies.

Notwithstanding these limitations, to our knowledge, this is the first study to apply highly multiplexed DSP to discriminate between EDAD and ODAD. The extent to which the many millions of COVID-19 survivors are at risk of developing pulmonary fibrosis is only beginning to be understood.²⁰ Importantly, many of the protein targets we have identified as being highly expressed at the early stages of DAD are amenable to therapeutic intervention with existing drugs or drugs in development. Hence, further exploration of these targets as potential regulators of DAD progression using preclinical models of SARS-CoV-2, as well as in other diseases associated with DAD, could provide an evidence base on which to conduct future intervention trials.

Author affiliations

¹York Biomedical Research Institute, Hull York Medical School, University of York, York, UK

²Newcastle University Translational and Clinical Research Institute, Newcastle upon Tyne, UK

³Department of Mathematics, University of York, York, UK

⁴Department of Cellular Pathology, Newcastle Upon Tyne Hospitals NHS Foundation Trust, Newcastle Upon Tyne, UK

⁵Wellcome Sanger Institute, Wellcome Genome Campus, Hinxton, UK

⁶Biosciences Technology Facility, University of York, York, UK

⁷Biosciences Institute, Newcastle University, Newcastle upon Tyne, UK

⁸Institute of Transplantation, Newcastle Upon Tyne Hospitals NHS Foundation Trust, Newcastle Upon Tyne, UK

Handling editor Vikram Deshpande.

Twitter Jimmy Tsz Hang Lee @thjimmylee

Acknowledgements The authors would like to acknowledge the tissue donors and their families for their contribution to medical science.

Contributors AJF, AF, OAB, DL, JTHL, NS and PMK contributed to the conception and design of the study. HA, GC, AF, BH and SJ generated samples and performed DSP analysis; LM and JM performed pathology guided ROI selection; JW and PMK conducted data analysis. All authors contributed to drafting the manuscript or critical review and all provided approval for submission.

Funding This work was funded by UK Research and Innovations/NiHR UK Coronavirus Immunology Consortium (UK-CIC; MR/V028448). PMK is also supported by a Wellcome Trust Senior Investigator Award (WT104726). OAB and JTHL were supported by Wellcome Trust Core Funding to the Sanger Institute. ICHTB is supported by the National Institute for Health Research (NIHR) Biomedical Research Centre based at Imperial College Healthcare NHS Trust and Imperial College London.

Disclaimer The funders had no role in the design or conduct of the study of the decision to publish. The views expressed are those of the author(s) and not necessarily those of the NHS, the NIHR or the Department of Health.

Competing interests None declared.

Patient consent for publication Not applicable.

Ethics approval Human samples used in this research project were partly obtained from the Newcastle Hospitals CEPA Biobank and their use in research is covered by Newcastle Hospitals CEPA Biobank ethics—REC 17/NE/0070. Additional human samples used in this research project were obtained from the Imperial College Healthcare Tissue Bank (ICHTB). ICHTB is approved by Wales REC3 to release human material for research (22/WA/0214). Additional human samples used in this research project were obtained from the ICECAP tissue bank of the University of Edinburgh. ICECAP is approved by the East of Scotland Research Ethics Service to release human material for research (16/ED/0084). Analysis of these samples at the

University of York was approved by the Hull York Medical School Ethics Committee (20/52).

Provenance and peer review Not commissioned; externally peer reviewed.

Supplemental material This content has been supplied by the author(s). It has not been vetted by BMJ Publishing Group Limited (BMJ) and may not have been peer-reviewed. Any opinions or recommendations discussed are solely those of the author(s) and are not endorsed by BMJ. BMJ disclaims all liability and responsibility arising from any reliance placed on the content. Where the content includes any translated material, BMJ does not warrant the accuracy and reliability of the translations (including but not limited to local regulations, clinical guidelines, terminology, drug names and drug dosages), and is not responsible for any error and/or omissions arising from translation and adaptation or otherwise.

Open access This is an open access article distributed in accordance with the Creative Commons Attribution 4.0 Unported (CC BY 4.0) license, which permits others to copy, redistribute, remix, transform and build upon this work for any purpose, provided the original work is properly cited, a link to the licence is given, and indication of whether changes were made. See: <https://creativecommons.org/licenses/by/4.0/>.

ORCID iD

Paul M Kaye <http://orcid.org/0000-0002-8796-4755>

REFERENCES

- 1 Centre JHCR. Available: <https://coronavirus.jhu.edu/map.html>
- 2 Li Y, Wu J, Wang S, et al. Progression to fibrosing diffuse alveolar damage in a series of 30 minimally invasive autopsies with COVID-19 pneumonia in Wuhan, China. *Histopathology* 2021;78:542–55.
- 3 Milross L, Majo J, Cooper N, et al. Post-mortem lung tissue: the fossil record of the pathophysiology and immunopathology of severe COVID-19. *Lancet Respir Med* 2022;10:95–106.
- 4 Nienhold R, Ciani Y, Koelzer VH, et al. Two distinct immunopathological profiles in autopsy lungs of COVID-19. *Nat Commun* 2020;11:5086.
- 5 Damiani S, Fiorentino M, De Palma A, et al. Pathological post-mortem findings in lungs infected with SARS-cov-2. *J Pathol* 2021;253:31–40.
- 6 Delorey TM, Ziegler CGK, Heimberg G, et al. COVID-19 tissue atlases reveal SARS-cov-2 pathology and cellular targets. *Nature* 2021;595:107–13.
- 7 Rendeiro AF, Ravichandran H, Bram Y, et al. The spatial landscape of lung pathology during COVID-19 progression. *Nature* 2021;593:564–9.
- 8 R: A language and environment for statistical computing. *R foundation for statistical computing*. Vienna, Austria [program], 2021.
- 9 pls: partial least squares and principal component regression. R package version 2.8-0 program. 2021.
- 10 pls: partial least squares and principal component regression. R package version 1.5-2 program. 2018.
- 11 Sing T, Sander O, Beerenwinkel N, et al. ROCr: visualizing classifier performance in R. *Bioinformatics* 2005;21:3940–1.
- 12 Dean MJ, Ochoa JB, Sanchez-Pino MD, et al. Severe COVID-19 is characterized by an impaired type I interferon response and elevated levels of arginase producing granulocytic myeloid derived suppressor cells. *Front Immunol* 2021;12.
- 13 Guo L, Schurink B, Roos E, et al. Indoleamine 2,3-dioxygenase (IDO) -1 and IDO-2 activity and severe course of COVID-19. *J Pathol* 2022;256:256–61.
- 14 Chilosi M, Poletti V, Ravaglia C, et al. The pathogenic role of epithelial and endothelial cells in early-phase COVID-19 pneumonia: victims and partners in crime. *Mod Pathol* 2021;34:1444–55.
- 15 Zhang B, Zhang Y, Xiong L, et al. CD127 imprints functional heterogeneity to diversify monocyte responses in inflammatory diseases. *J Exp Med* 2022;219:e20211191.
- 16 ElTanbouly MA, Zhao Y, Schaafsma E, et al. Vista: a target to manage the innate cytokine storm. *Front Immunol* 2020;11.
- 17 Bittmann I, Müller C, Behr J, et al. Fas/FasL and perforin/granzyme pathway in acute rejection and diffuse alveolar damage after allogeneic lung transplantation—a human biopsy study. *Virchows Arch* 2004;445:375–81.
- 18 Laplante M, Sabatini DM. Mtor signaling in growth control and disease. *Cell* 2012;149:274–93.
- 19 Saito R, Yanai M, Miki Y, et al. Immunohistochemical evidence for the association between attenuated mTOR signaling and diffuse alveolar damage, a fatal lung complication. *Tohoku J Exp Med* 2014;234:67–75.
- 20 Tarraso J, Safont B, Carbonell-Asins JA, et al. Lung function and radiological findings 1 year after COVID-19: a prospective follow-up. *Respir Res* 2022;23:242.

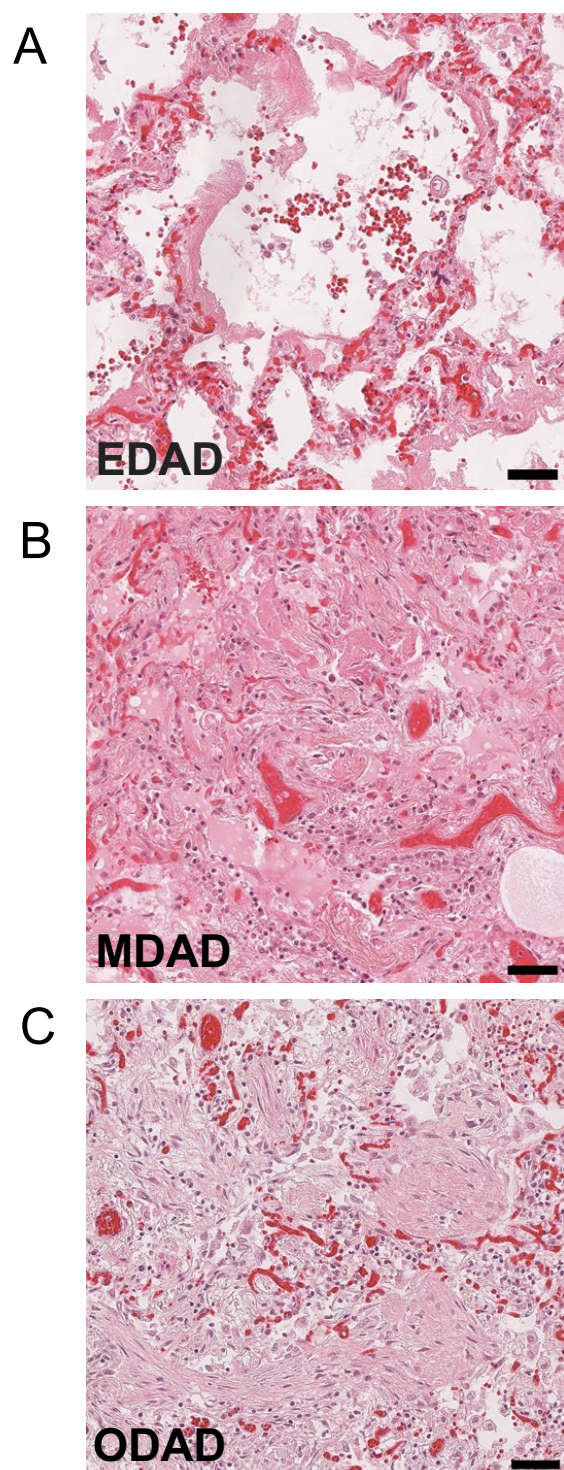


Figure S1. Representative images showing DAD progression

A) Exudative DAD (EDAD). **B)** mixed DAD (MDAD). **C)** organising DAD (ODAD).

Scale bar = 50µm